



HAL
open science

Between electron delocalization and low-lying excited states of BN-doped aromatic hydrocarbons

Chen Zhang, Anna Chrostowska, Shih-Yuan Liu, Panaghiotis Karamanis,
Nicolás Otero

► **To cite this version:**

Chen Zhang, Anna Chrostowska, Shih-Yuan Liu, Panaghiotis Karamanis, Nicolás Otero. Between electron delocalization and low-lying excited states of BN-doped aromatic hydrocarbons. *Chemical Physics Letters*, 2023, 825, pp.140615. 10.1016/j.cplett.2023.140615 . hal-04109523

HAL Id: hal-04109523

<https://univ-pau.hal.science/hal-04109523>

Submitted on 30 May 2023

HAL is a multi-disciplinary open access archive for the deposit and dissemination of scientific research documents, whether they are published or not. The documents may come from teaching and research institutions in France or abroad, or from public or private research centers.

L'archive ouverte pluridisciplinaire **HAL**, est destinée au dépôt et à la diffusion de documents scientifiques de niveau recherche, publiés ou non, émanant des établissements d'enseignement et de recherche français ou étrangers, des laboratoires publics ou privés.

Between electron delocalization and low-lying excited states of BN-doped aromatic hydrocarbons.

Chen Zhang,^a Anna Chrostowska,^a Shih-Yuan Liu,^{a,b} Panagiotis Karamanis,^{a*} and Nicolás Otero^c

^aE2S UPPA, CNRS, IPREM, Université de Pau et des Pays de l'Adour, 64053 Pau, France

^bDepartment of Chemistry, Boston College, Chestnut Hill, Massachusetts 02467-3860, United States

^cDepartment of Physical Chemistry, University of Vigo, Lagoas-Marcosende s/n, 36310.Vigo, Spain

Corresponding author: P. Karamanis: panagiotis.karamanis@univ-pau.fr

Abstract

The current study focuses on the impact of BN doping on the first singlet/triplet excited-states of simple BN-doped polyaromatic hydrocarbons. Our results, obtained on BN-phenanthrenes and other PHs, demonstrate that the BN-doping effect on the first single and triplet excited states of the parental hydrocarbon heavily depends on the electron delocalization between the carbon atoms being replaced. Specifically, it is revealed that dramatic changes occur when single CC-bonds of low-electron-delocalization are replaced. On the other hand, the replacement of CC-bonds of higher electron-delocalization, such as aromatic and/or double-CC-bonds, results in weaker and in some cases negligible excited state variations.

Introduction

BN-doped polycyclic aromatic hydrocarbons (PAHs)[1–5] are a class of organic heteroaromatic compounds that contain boron-nitrogen (B-N) units fused into their framework. These compounds have been of interest for their unique physical and chemical properties, which differ from their all-carbon counterparts. BN-doped hydrocarbons can be synthesized by replacing one or more carbon-carbon (CC) bonds in a hydrocarbon with a B-N unit. This substitution can affect the electronic structure, optical, and electrochemical properties of the resulting compound. Therefore, by replacing one or more CC bonds in a simple polyaromatic hydrocarbon (PAH) with polarized boron-nitrogen (B-N) units, it is possible to create a new “chemical space”[6] of BN-doped isosteres. This approach provides a method for creating diversity through varying the locations of doping sites and orientations of BN units offering alternative routes to engineer novel organic compounds with unique physical and chemical properties for various technological applications. Such application might involve optoelectronics[7–9], energy[10], and materials science.[6] In particular, such species have been considered for applications in organic solar cells[7,11] of improved energy conversion efficiency.

One of the key factors in this realm is the effect of BN doping on the excited states of simple aromatic species, which refers to the energy levels generated by the absorption of light or other forms of electromagnetic radiation. Understanding the excited-state properties of these compounds is crucial for the design and development of new molecules with tailored physical and chemical properties for various technological applications. Despite the intense synthetic activity in this subject, little work has been dedicated to the systematic investigation on the excited states of simple BN-doped aromatic hydrocarbons. Most of the reported studies deal with the investigation of HOMO-LUMO gaps [12,13] and ionization energies[14] which provide only indirect qualitative insights about BN doping effects on the excited state quantum transitions in aromatic hydrocarbons.

In this letter, we provide a systematic study on the vertical and adiabatic excited states of BN-doped phenanthrenes paying particular attention to bonding and electron delocalization. Phenanthrene ($C_{14}H_{10}$), frequently used in organic chemistry as a modular building block, is a reference planar polycyclic aromatic hydrocarbon (PAH) consisting of three fused benzene rings in a linear arrangement.. What is interesting about this molecule is that it comprises all common types of bonding (i.e. single, aromatic, and double bonds). This feature is very convenient for structure-property studies because it allows us to directly compare the effect of BN doping on these bonds. So far, out of the sixteen possible BN doped

phenanthrenes, six have been synthesized and studied with respect to their electronic structure and optical properties (see ref [15] and references therein). The properties of the remaining eleven possible BN doped phenanthrenes are practically unknown.

To study the effect of BN-substitution of the excited states of BN-doped phenanthrenes we considered the following quantities:

$$S_1^{A,V} = E_{\text{excited state singlet}}^{A,V} - E_{\text{ground state}} \quad (1)$$

$$T_1^{A,V} = E_{\text{excited state triplet}}^{A,V} - E_{\text{ground state}} \quad (2)$$

$$\Delta S_1^{A,V} = S_1^{A,V}(\text{BN}) - S_1^{A,V}(\text{Phen}) \quad (3)$$

$$\Delta T_1^{A,V} = T_1^{A,V}(\text{BN}) - T_1^{A,V}(\text{Phen}) \quad (4)$$

In the above equations $E_{\text{ground state}}$ stands for the ground state singlet electronic energy of each system, while $E_{\text{excited state singlet}}^A$ and $E_{\text{excited state triplet}}^A$ represent the electronic molecular energies of the first singlet and triplet state, computed in the singlet equilibrium nuclear geometries of each system. On the other hand, $E_{\text{excited state singlet}}^V$ and $E_{\text{excited state triplet}}^V$ stand for the electronic energy of the first singlet and triplet excited states in their equilibrium geometries. Therefore, S_1^A (T_1^A) and S_1^V (T_1^V) are the adiabatic, and vertical singlet (triplet) excitation energies of each system, respectively. $\Delta S_1^{A,V}$ and $\Delta T_1^{A,V}$ are the difference between $S_1^{A,V}$ ($T_1^{A,V}$) excitation energies of the BN doped species and the corresponding quantities of pristine phenanthrene. The later quantities will serve here as a measure of the BN-doping impact on the excited state properties of pristine phenanthrene. In brief, large absolute values of $\Delta S_1^{A,V}$ and $\Delta T_1^{A,V}$ should denote a significant impact on the excited states of BN doping. Also, positive values of $\Delta S_1^{A,V}$ and $\Delta T_1^{A,V}$ correspond to species featuring larger $S_1^{A,V}$ and $T_1^{A,V}$ excitation energies than phenanthrene and *vice versa*. It is important to stress here that the aim of this letter is not to reproduce experimental data or to provide reference excited state energies of the studied systems, but to conclude to handy structure property correlations that can be utilized in synthesis of BN doped PAHs with distinct photophysical properties.

Our work is organized as follows. First, we revisit the bonding of pristine phenanthrene focusing on electron delocalization in rings and between CC bonds. To accomplish this task, we relied on calculations of six-center delocalization indices (6cDIs) accounting for the multicenter electron delocalization. As it will be shown in the following pages, this sort of analysis is of essential importance to rationalize the doping effects on the excited state of these BN-doped species. In the second part of this work, we discuss the

difference between the vertical and adiabatic excited states of all possible monosubstituted BN-phenanthrenes and the parental all-carbon hydrocarbon. Lastly, we examine the robustness of the property correlations found in the reference molecule of phenanthrene to other polyaromatic hydrocarbons of various bonding patterns and sizes.

Computational details

All computations presented in this work have been carried out with the GAUSSIAN 16[16] suite of programs. To determine molecular equilibrium geometries, we relied on the post-Hartree-Fock coupled cluster singles and doubles (CCSD) approximation and two DFT functionals PBE0 and B3LYP. We also utilized the range-separated version of the latter hybrid functional designed to address limitations in the case of charge-transfer excited states, namely, CAM-B3LYP[17]. Singlet excited state energy calculations in this study were performed using the equation of motion coupled-cluster method (EOM-CCSD)[18] and time-dependent density functional theory (TD-DFT)[19] with the previously mentioned DFT functionals. The first triplet state of all molecules has been computed with open shell DFT (UDFT) and CCSD (UCCSD) approximations. The reliability of the CCSD closed shell computations been assessed by carrying out the so-called T1 diagnostic introduced by Lee and Taylor [20] as a measure of the importance of higher-order excitations (e.g., triple and quadruple excitations) and of the importance of non-dynamical electron correlation in the CC wavefunction. In all closed-shell systems investigated here, the obtained T1 diagnostics were found to be lower than 0.02. Depending on the method we used for the calculation of the properties of interest we used the appropriate basis set. In short, all computations using Density Functional Theory (DFT) have been carried out with the 6-311G(d,p) basis sets. On the other hand, (EOM)CCSD calculations have been performed using the cc-pVDZ correlation consistent basis sets. This applies to both adiabatic and vertical excitations. For the latter vertical transitions, the aug-cc-pVDZ basis set was additionally utilized. This was done to gain some insight into the potential impact of the basis set on (EOM)-CCSD calculations. Furthermore, we carried out computations of intrinsic polarizability density distributions and electron delocalization. The term "intrinsic" atomic polarizability refers to the contribution of a specific atom within a molecule to its overall molecular polarizability. Two authors of this study in a series of articles (see refs [21–23] and references therein) demonstrated the feasibility of visualizing intrinsic atomic polarizabilities as density-like representations using atomic partitioning schemes, such as the Fractional-Occupation-Hirshfeld-Iterative (FOHI) [24,25] method, which takes into account the actual electron density of the molecule. In the case of (poly)aromatic hydrocarbons, these visual representations accurately reproduce the corresponding superposed Clar's formulas[26]. Finally, we calculated the electron delocalization indices between bonds and within doped and all carbon six-member rings. For this task, we

computed two (2cDIs) and six-center delocalization indices (6cDIs) accounting for the multicenter electron delocalization and aromaticity[27] via a QTAIM-based scheme[28] via the Generalized Population Analysis (GPA).[29] The Fortran implementation program is available in the public repository <https://github.com/nom05/ndeloc> under GPL3 license.[30]

Results and Discussion

We begin our analysis with **Figure 1a**, illustrating the FOHI two- and six-center electron delocalization indices for pristine phenanthrene, along with mean intrinsic polarizability positive densities (MIP+) mapped onto its molecular plane. In the same figure, we also show the FOHI atomic charges of each atom computed at the same level of theory. The nuclear equilibrium geometry of pristine phenanthrene has been obtained via geometry optimization at the CCSD/cc-pVDZ level of theory. The respective reference structural are given in supporting material together with the rest of the molecules considered (**Table S5**).

The six-center-electron (6cDI) delocalization indices, displayed at the center of carbon rings **A** and **B**, confirm earlier studies[31,32] suggesting that phenanthrene is composed of two symmetry-equivalent carbon rings (marked with the letter **A**) with a high degree of electron delocalization ($5.6 \cdot 10^{-3}$ au) and a hexagon (marked as **B**) of significantly smaller electron delocalization ($1.8 \cdot 10^{-3}$ au). In terms of Clar's theory of aromaticity, hexagons **A** and **B** should be considered as aromatic and non-aromatic sextets, respectively. Therefore, phenanthrene can be described as a planar biphenyl molecule with its two aromatic sextets bridged by a double bond formed between carbon atoms **9** and **10**. The nature of the aforementioned bond is demonstrated through the calculated FOHI two-center delocalization indices (2cDI). The computations reveal that the (**9,10**) carbon-carbon (CC) bond exhibits the highest 2cDI, reaching an approximate value of 1.7 au. On the contrary, the (**4b,4a**) CC bond has the lowest 2cDI, which is close to one. This characteristic is typically found in single CC bonds. In the context of the two aromatic hexagons in phenanthrene, there's a significant disparity in the calculated 2cDIs for the bonds that form symmetry-equivalent hexagons **A** and **B**. Specifically, the highest 2cDIs are predicted to occur between carbon atoms (**4,3**)/(**6,5**) and (**1,2**)/(**7,8**). In contrast, the lowest 2cDI is observed between (**4a, 4**) and (**4b, 5**).

The MIP+ densities representing the local variation in the polarizability of the electron cloud of a molecule [33] validates the picture obtained by the computed 6cDIs and 2cDIs. As seen, the less delocalized hexagon **B** exhibits a discontinuous distribution of MIP+ densities, with the highest values localized in the vicinity (**9,10**) carbon-carbon bond. In contrast, the two symmetry-equivalent carbon rings feature diffuse MIP+ densities distributed between all of their six atoms. Furthermore, it is seen that the distribution of the MIP+ densities within the aromatic rings is less homogeneous than those obtained for the reference molecule of

benzene[26] or larger structures of planar polyaromatic carbons such as graphene flakes[34,35]. The observed deviation aligns very well with the different electron delocalization of the CC bonds forming the two aromatic sextets of phenanthrene.

Figure 1b illustrates the structures of all sixteen BN doped phenanthrene, selected FOHI atomic charges, scalar dipole moments, and the corresponding vector directions. A first glance quickly suggests that BN doping brings significant changes in the direction and the magnitude of the dipole moment with respect to the free phenanthrene molecule which belongs to the C_{2v} point group of symmetry, with the C_2 symmetry axis passing from the center of its molecular plane (see dotted lines in **Figure 1b**). In all cases, the molecular dipole moments of the doped species are quasi-parallel to the axis of the BN bond pointing from the boron to the nitrogen atom. The changes brought by the BN substitution on the dipole moment magnitude of phenanthrene are massive compared to the permanent dipole moment of pristine phenanthrene (0.015 Debye at the same level of theory). The most polar BN phenanthrene isosteres are BN(**4a,4b**) and BN(**8a,9**)/BN(**9,8a**) bearing dipole moments lying higher than 3.0 Debye. In these species, the BN unit replaces CC bonds of small electron delocalization. On the other hand, the weakest polar molecule is BN(**9,10**), in which the BN unit replaced the bridging double CC bond. Furthermore, the FOHI atomic charges reveal that the position of the nitrogen atoms is of great importance for their charges. The smallest negative atomic charges are observed in species in which the nitrogen atom, in addition to boron, is bonded to two carbon atoms. This is because the nitrogen atom is surrounded by two carbon atoms, closer in electronegativity than boron and hydrogen. For this reason, nitrogen is not able to withdraw sufficient electrons. Conversely, a more substantial negative charge is predicted when N is bonded to one H atom and one carbon, as expected according to Pauling's electronegativity scale. Lastly, the positive atomic charges on B atoms exhibit smaller variations with respect to their position in the molecular framework than those observed in N.

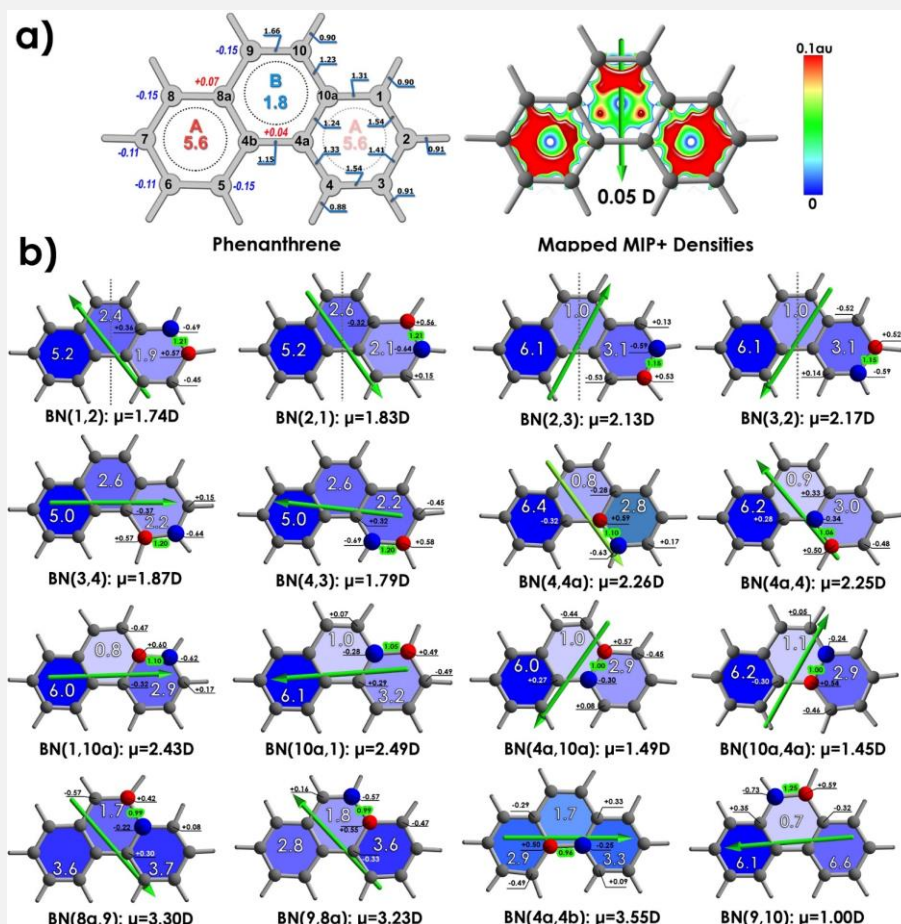


Figure 1. **a)** (Left) atom numbering of phenanthrene (used for the nomenclature of the considered systems in Figure 1b), FOHI 2-center electron delocalization indices (underscored values) representing the delocalization of the electron density between two atoms. Numbers on each hexagon are the 6-center delocalization indices representing the electron delocalization in rings. Numbers in italics are the FOHI atomic charges on each heavy atom. (Right) Mapped surface representing the mean dipole positive polarizability densities (MIP+) of phenanthrenes within the limits of each carbon ring. Red/Blue contours represent high/low MIP+ densities. All computations have been performed at the B3LYP/6-311G(d,p) level of theory. **b)** Molecular structures of all BN doped phenanthrenes, dipole moment vectors, and scalar dipole moment values given in Debye, FOHI atomic charges on selected atoms, and 6-center-delocalization indices (numbers of large fonts). Dotted lines in the first row correspond to the dipole moment axis of the pristine molecule of phenanthrene ($\mu=0.05$ Debye). Numbers in the green background correspond to 2-center-delocalization indices of the incorporated BN bond. Electron density partitioning computations have been performed on CCSD/cc-pVDZ equilibrium nuclear geometries with the B3LYP/6-311G(d,p) functional. Dipole moment vectors and scalar dipole moment values have been computed with the B3LYP/6-311+G(d,p) method applied on equilibrium nuclear geometries obtained at the same level of theory. In the representation of the dipole moment vectors, we adopted the notation used in physics, hence the dipole moment vector points from (-) to (+). All FOHI 2-center electron delocalization indices are in au, while the 6cDIs are in au and multiplied by 10^3 .

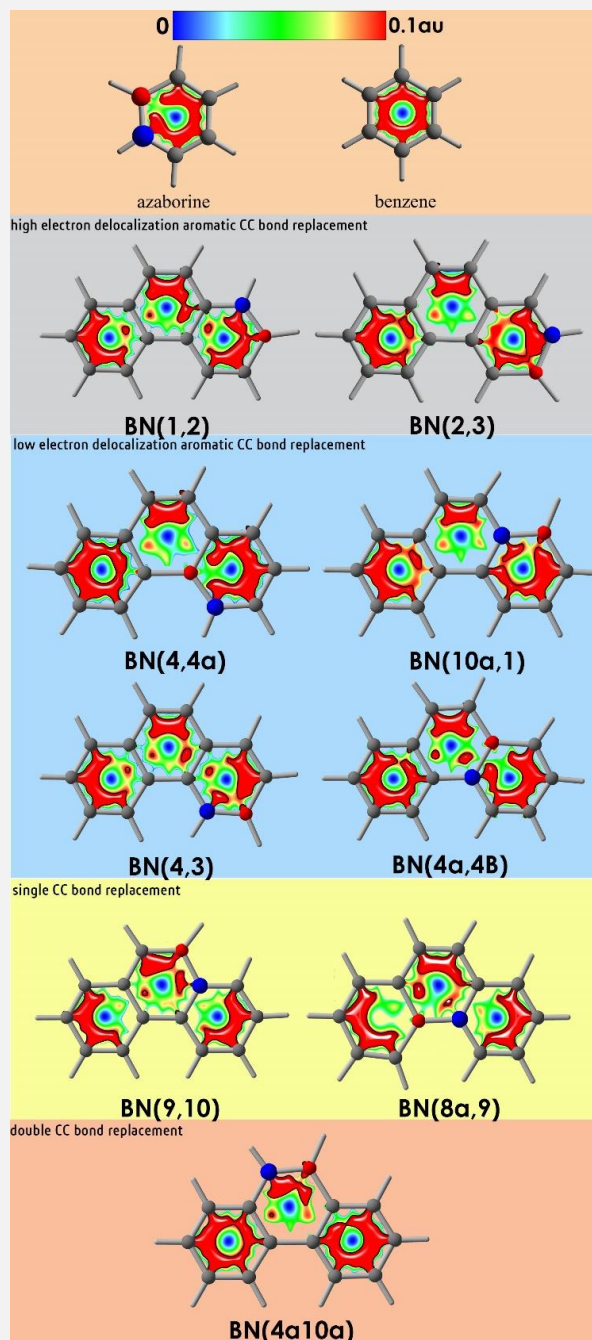


Figure 2. MIP+ densities of selected BN doped phenanthrenes computed at the B3LYP/6-311G(d,p) level of theory applied on CCSD/cc-pVDZ optimized geometries. For the sake of comparison, we have also plotted the corresponding densities of the free molecules of benzene and azaborine.

Turning our attention to the character of the incorporated BN unit, we see that all BN bonds feature smaller electron delocalization indices with respect to the corresponding CC bonds of pure phenanthrene. The lowest indices of the BN bonds are spotted when the BN unit replaces a CC bond of low electron delocalization and vice-versa. This is an interesting effect because it implies that the bonding of the incorporated BN unit carries traces of the CC bond character that has been replaced. For instance, the highest electron delocalization between B and N atoms is spotted in BN(9,10), in which the BN unit replaced the double bond of its parental molecule. The 6cDIs shown at the center of each hexagon of the doped species suggest BN doping on a single bond (cases BN(8a,9)/(9,8a) and BN(4a,4b)) decreases the ring electron delocalization of both aromatic sextets of phenanthrene. On the other hand, BN doping on the double CC bond bridging the two aromatic hexagons (case BN(9,10)) increases the electron delocalization in both aromatic sides of the phenanthrene. For the rest of BN isosteres in which the BN units replace “aromatic” CC bonds, we see that BN doping drastically decreases the electron delocalization of the doped ring. At the same time, some minor changes are also triggered in the electron delocalization of the non-doped ring. The most substantial decrease occurs when the BN unit replaces most delocalized bonds in their pristine counterpart, namely, (1,2)/(2,1) and (3,4)/4,3). Hence, reducing the delocalization in these bonds via BN substitution impacts the delocalization of the whole ring. A visual representation of how the BN unit affects the most electron-delocalized parts of the molecules in terms of MIP+ densities is illustrated in **Figure 2**. It is evident that there is a notable differentiation between MIP+ densities located in aromatic rings near a BN unit, with respect to the bonding properties of the substituted CC bond. The observation suggests that when BN takes the place of an aromatic bond with low electron delocalization, the MIP+ densities surrounding the boron atoms become disrupted. Conversely, this effect is less noticeable or non-existent in the scenario where an aromatic CC bond with higher 2cDIs, is replaced. Finally, we performed a brief stability test between all BN doped phenanthrenes we considered in this study. The results obtained (refer to **Table S6** of supporting material) indicate that the most stable isomer is BN(9,10), which also exhibits the greatest electron delocalization in its rings. Conversely, the least stable isomers are BN(8a,9) and BN(4a,4b). According to the B3LYP/6-311G(d,p) level of theory, these are found to be 26 and 22.4 kcal/mol higher in energy, respectively. The electron delocalization within the rings of these two isomers is less intense than in the remaining BN-doped phenanthrenes considered in this study. This finding is consistent with the general trend in chemistry where aromaticity serves as an indicator of stability in organic molecules.

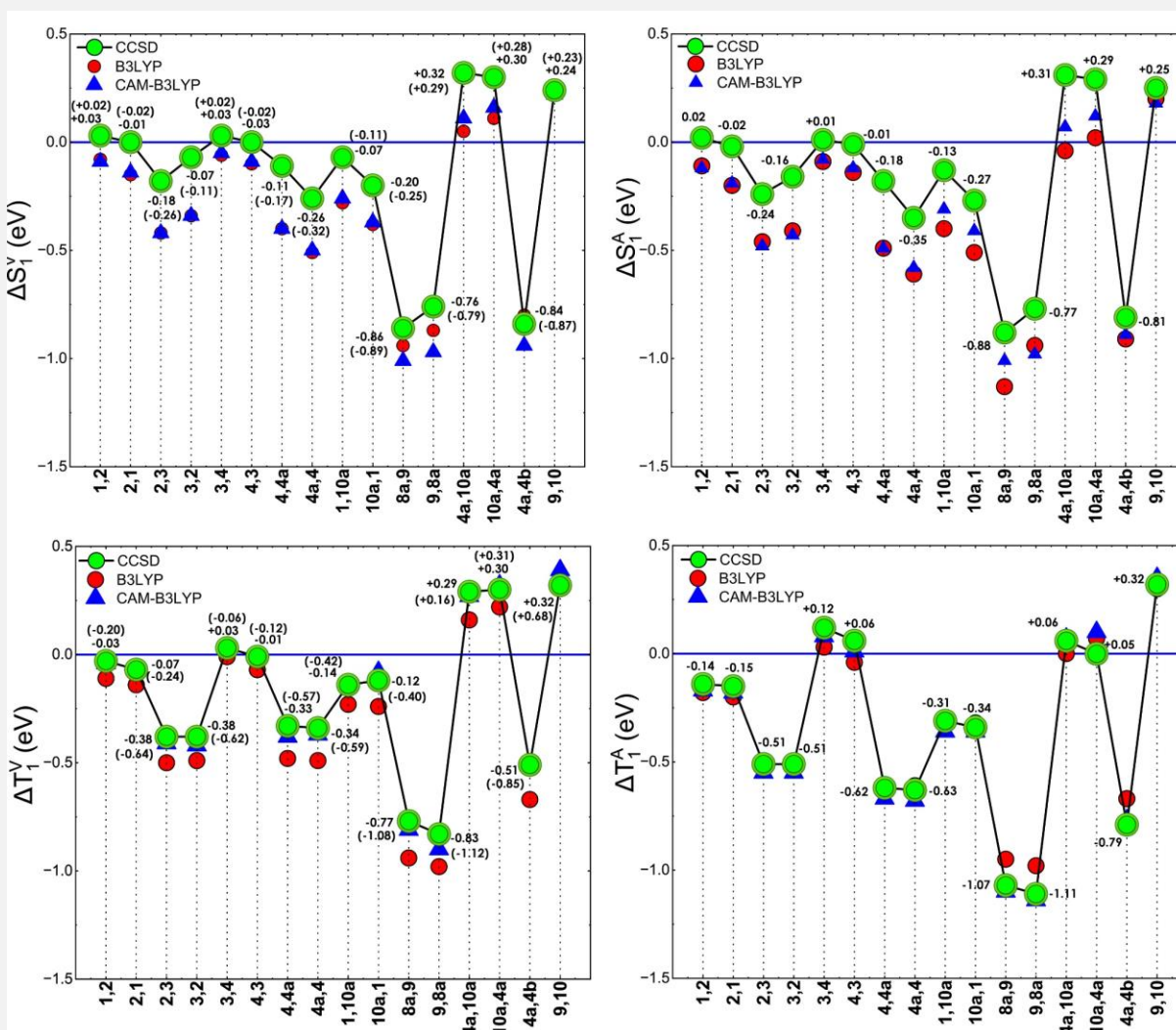


Figure 3. Variation of $\Delta S_1^{A,V}$ and $\Delta T_1^{A,V}$ energy differences computed with the CCSD/cc-pVDZ, (CAM-) B3LYP/6-311G(d,p) methods. All values correspond to equilibrium nuclear geometries obtained at the corresponding levels of theory. Numbers on each plot correspond to (EOM)CCSD/(aug)-cc-pVDZ $\Delta S_1^{A,V}$ and $\Delta T_1^{A,V}$ values.

Figure 3 shows the variation of the quantities defined in eq. (1)-(4) as a function of boron nitrogen doping site computed at various levels of theory. A first glance readily suggests that the effect of BN doping on the low-lying excited states of phenanthrene heavily depends on the doping site in terms of size and sign. On the other hand, the orientation of the BN unit has a minor influence on the computed $\Delta S_1^{V,A}$ and $\Delta T_1^{V,A}$ values. This is evident from the orientational isomers BN(1,2)/(2,1) and BN(2,3)/(3,2), which possess similar absolute CCSD $\Delta S_1^{V,A}$ and $\Delta T_1^{V,A}$ values. The corresponding excited state energy differences are listed in **Table I**. A brief analysis of each transition, by means of natural transition orbitals is given in supporting material. In the majority of cases the transition between ground and first singlet, triplet energies can be sufficiently described by transitions between the respective highest(lowest) occupied(unoccupied)

molecular orbitals (HOMO and LUMO). Finally, if we compare the vertical and adiabatic energy differences, it becomes evident that $\Delta S_1^V \sim \Delta S_1^A$. This observation might prove especially useful for investigations focusing on singlet fission processes.[32,33]

The largest absolute $\Delta S_1^{V,A}$ and $\Delta T_1^{V,A}$ differences are observed in species BN(**8a,9**)/(**9,8a**) and BN(**4a,4b**). Depending on the level of approximation applied, the obtained differences vary from 0.8 to 1.0 eV for either the singlet or triplet vertical excitation energies. Similar energy changes are observed in the case of the adiabatic differences between the ground and the first singlet and triplet states. On the other hand, the smallest ΔS_1^V and ΔT_1^V absolute values at the CCSD level of theory are predicted for isosteres BN(**1,2**)/(**2,1**) BN(**3,4**)/(**4,3**) BN(**1a, 10**). At the respective levels of theory, we obtained ΔS_1^V and ΔT_1^V differences below the threshold of 0.05 eV. Therefore, no significant changes in the singlet and triplet energies of the parental phenanthrene should be expected if BN doping is applied in these bonds. See, for instance, the CCSD values obtained for BN(**2,1**) and BN(**4,3**). Lastly, our computations predict that BN doping brings intermediate changes on their vertical singlet and triplet excited states for the remaining isosteres of phenanthrene. At the CCSD level of theory, the observed changes may vary between 0.1 and 0.35 eV.

Regarding the performance of the methods used, we observe that the CCSD approximation, the most accurate method employed in this study, produces the smallest ΔS_1^V and ΔT_1^V values compared to the conventional DFT functionals we considered. On the other hand, the less expensive CAM- and B3LYP/6-311G(d,p) methods yield somewhat overestimated differences with respect to the CCSD/(aug)-cc-pVDZ results but successfully predict the relevant signs. For the cases in which the singlet and triplet energy differences between the doped phenanthenes and their pristine counterpart lie close to zero, it would be difficult to determine the exact sign of $\Delta S_1^{V,A}$ and $\Delta T_1^{V,A}$ quantities. For this task, higher levels of approximation and richer basis sets are required, a task that is beyond the scope of this article which focuses on relative trends. Finally, we computed ΔT_1^V quantities within the EOM-CCSD/cc-pVDZ level of theory. The obtained results reproduced very well those depicted in **Figure 2**, which have been obtained from the difference in energy between the ground state singlet and the energy of the triplet state computed at the equilibrium geometry of the singlet.

Table I. Vertical and adiabatic singlet and triplet excitation energies computed at various levels of theory. All energy values are given in eV.

Molecule	S_1^V			S_1^A			T_1^V			T_1^A		
	B3L ^a	CAM ^b	EOM ^c	B3L	CAM	EOM	B3L	CAM	CC ^d	B3L	CAM	CC
Phenanthrene ^e	3.99	4.35	4.18	3.86	4.18	4.00	2.88	2.64	3.02	2.77	2.84	2.87
BN(1,2)	3.91	4.26	4.21	3.75	4.06	4.02	2.77	2.60	2.99	2.59	2.67	2.73
BN(2,1)	3.84	4.21	4.18	3.66	3.99	3.98	2.74	2.57	2.95	2.57	2.66	2.72
BN(2,3)	3.57	3.93	4.00	3.4	3.70	3.76	2.38	2.23	2.64	2.24	2.29	2.36
BN(3,2)	3.65	4.01	4.11	3.45	3.75	3.84	2.39	2.22	2.64	2.25	2.29	2.36
BN(3,4)	3.93	4.03	4.21	3.77	4.10	4.01	2.87	2.67	3.05	2.80	2.92	2.99
BN(4,3)	3.89	4.26	4.18	3.72	4.06	3.99	2.81	2.63	3.01	2.73	2.85	2.93
BN(4,4a)	3.59	3.95	4.07	3.37	3.69	3.82	2.40	2.26	2.69	2.16	2.17	2.25
BN(4a,4)	3.48	3.85	3.92	3.25	3.6	3.65	2.39	2.27	2.68	2.16	2.16	2.24
BN(1,10a)	3.71	4.09	4.11	3.46	3.87	3.87	2.65	2.50	2.88	2.46	2.48	2.56
BN(10,a1)	3.61	3.98	3.98	3.35	3.77	3.73	2.64	2.56	2.90	2.45	2.48	2.53
BN(8,a9)	3.05	3.34	3.32	2.73	3.17	3.12	1.94	1.83	2.25	1.82	1.74	1.80
BN(9,8a)	3.12	3.38	3.42	2.92	3.20	3.23	1.90	1.74	2.19	1.79	1.70	1.76
BN(4a,10a)	4.04	4.46	4.5	3.82	4.25	4.31	3.04	2.91	3.31	2.77	2.91	2.93
BN(10a,4a)	4.10	4.51	4.48	3.88	4.30	4.29	3.10	2.96	3.32	2.84	2.94	2.92
BN(4a,4b)	3.19	3.41	3.34	2.95	3.29	3.19	2.21	2.13	2.51	2.10	2.07	2.08
BN(9,10)	4.21	4.57	4.42	4.06	4.36	4.25	3.21	3.03	3.34	3.07	3.19	3.19

^a B3LYP/6-311G(d,p)

^b CAM-B3LYP/6-311G(d,p)

^c EOM-CCSD/cc-pVDZ

^d UCCSD/cc-pVDZ

^e Exp S_1^A 3.63 eV[39], Theoretical S_1^V MP2/CC2/aug-cc-pVDZ 3.97 eV[40]

A careful comparison of the values listed in **Table I** reveals that the largest absolute $\Delta S_1^{V,A}$ and $\Delta T_1^{V,A}$ differences are observed in species BN(**8a,9**)/(**9,8a**) and BN(**4a,4b**). Depending on the level of approximation applied, the obtained differences vary from 0.8 to 1.0 eV for either the singlet or triplet vertical excitation energies. Similar changes are observed in the case of the adiabatic energy differences between the ground and the first singlet and triplet states. On the other hand, the smallest ΔS_1^V and ΔT_1^V absolute values at the CCSD level of theory are predicted for isosteres BN(**1,2**)/(**2,1**) BN(**3,4**)/(**4,3**) BN(**1a,10**). At the respective levels of theory, we obtained ΔS_1^V and ΔT_1^V differences below the threshold of 0.05 eV. Therefore, no significant changes in the singlet and triplet energies of the parental phenanthrene should be expected if BN doping is applied in these bonds of the parental all-carbon aromatic hydrocarbon.

After the above comparative analysis let us now revisit the bond delocalization data displayed in **Figure 1a** and contrast them to the results obtained for $\Delta S_1^{V,A}$ and $\Delta T_1^{V,A}$. It is revealed that the largest ΔS_1^V and ΔT_1^V differences occur when the BN unit is incorporated in bonds of small 2cDIs, namely, bonds (**8a,9**)/(**9,8a**) and (**4a,4b**). In striking contrast, the replacement of bonds belonging to aromatic sextets as the latter have been confirmed by the computed 6cDIs, deliver considerably smaller changes. See for instance the, ΔS_1^V and ΔT_1^V of species in which the BN unit replaces bonds (**1,2**) and (**3,4**) belonging to the one of the two equivalent aromatic sextets of phenanthrene. These bonds are the ones identified with the higher electron delocalization within each aromatic sextet. The performed excited state computations clearly suggest that BN doping in these bonds brings negligible changes on the first singlet and triplet excitation energies compared to the parental pristine molecule.

A deeper analysis of the obtained excited state outcomes reveals a correlation between electron delocalization in bonds and excitation energies, albeit partially, in species where one of their aromatic bonds has been substituted with a BN unit. Compare for instance, species BN(**1,2**) and BN(**2,3**) in which the BN units have replaced phenanthrene's aromatic bonds (**1,2**)/(2cDI=1.54e) and (**2,3**)/(2cDI=1.41e). In accord with above trend, the CCSD approximation predicts that $|\Delta S_1^V[\text{BN}(\mathbf{1,2})]|$ is about 0.15 eV smaller than $|\Delta S_1^V[\text{BN}(\mathbf{2,3})]|$, while $|\Delta T_1^V[\text{BN}(\mathbf{1,2})]|$ is about 0.35 eV smaller than $|\Delta T_1^V[\text{BN}(\mathbf{2,3})]|$. Hence, for this pair of structures BN incorporation on less delocalized CC bonds brings larger ΔS_1^V and ΔT_1^V energy differences than BN doping on a CC bond of high electron delocalization degree. A similar trend holds for species BN(**10a,1**) and BN(**1,10a**) in which phenanthrene's substituted bond is less delocalized than bonds (**1,2**) and (**2,3**). On the other hand, this correlation does not hold if we compare BN(**10a,1**)/(**1,10a**) with BN(**2,3**)/(**3,2**). In this case, the more delocalized bond is the one that brings a larger effect on the respective energy differences. A comparable discrepancy is observed in the case of the aromatic bond (**4a,10a**), with

its 2cDI (1.24e) being very close to the one computed for bond (10a,1) (1.23e), which in classical organic chemistry is considered single. A similar variation is found when comparing bonds (10a,1) and (2,3). The absence of a direct correlation in this case implies that additional effects should be considered to completely elucidate the correlation between the effect of BN doping on the excited states of phenanthrene and the character of the replaced CC bond. For instance, we refined the bonding analysis by determining the 2cDIs based on the density of the π -orbitals (2 π cDI). The obtained results suggested that bond (**4a,10a**) features a 2 π cDI value of 0.34e, while the corresponding quantity for bond (**10a,10**) is only 0.24e. On the other hand, 2cDIs for bonds (**10a,1**) and (**2,3**) are found to be almost equal (~ 0.30). In the latter case, one should consider possible mesomeric effects stemming from interactions with rest of the molecule that can be also vary depending on the position of the N and boron atoms that could play a role in the observed deviations. For example, we see that the BN incorporation at positions (**2,3**)/(**3,2**) equally decreases the delocalization in rings A and B, regardless of the orientation of the BN unit. This is not the case for the replacement of bond (**10a,1**), as different BN orientations result in different 6cDIs between these two rings. Lastly, we have also conducted further analysis on the energy difference between the first singlet and first triplet excited states. Our findings suggest that that BN doping in phenanthrene does not bring significant changes to the energy differences between the S_1 and T_1 states. The triplet and singlet excited states are separated by considerable energy differences, often exceeding 1 eV, implying a reduced probability of singlet triplet interactions. On the other hand no clear correlation between electron delocalization and energy differences between the S_1 and T_1 states was detected.

Up to this point, our computations on BN doped phenanthenes indicated that the effect of BN doping on its vertical and adiabatic excited state energies can be intuitively predicted under the condition that the BN unit replaces bonds of significant differences in electron delocalization. To test the robustness of the revealed relationship between the excitation energies of the singlet excited states and bonding, we performed the following computational experiment. We selected six different BN aromatic hydrocarbons (**Figure 4**) with varying sizes and bonding patterns and replaced their single, aromatic, and double bonds with BN units. We predicted the bond character in each case based on conventional principles of Clar's theory of aromaticity. For instance, the molecule of pyrene is equivalent to phenanthrene, featuring two aromatic and non-aromatic rings and one and two single and double CC bonds, respectively. Meanwhile, perylene can be seen as a naphthalene dimer connected by two single bonds. Hexabenzocoronene is a "claromatic"[38] planar polyaromatic molecule belonging to the family of nanographenes in which the π -electrons are localized in π -sextets, separated by non-aromatic rings. The geometries of these trial systems have been optimized at B3LYP/6-311G(d,p) level of theory and the respective vertical singlet quantum transitions have been obtained by TD-B3LYP computations using the same basis set. The energy

differences depicted in **Figure 4** confirm that the substitution of a single CC bond with a BN delivers larger ΔS_1^V differences between the parent molecule and the replacement of an aromatic double bond.

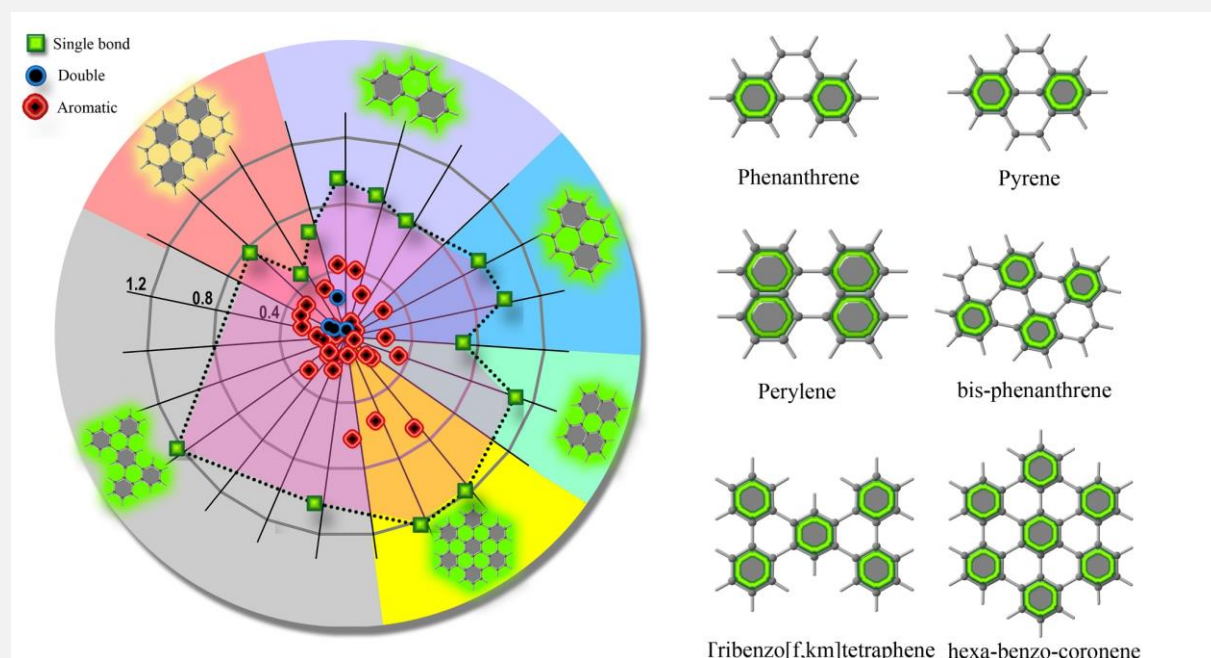


Figure 4. $|\Delta S_1^V|$ of six different BN doped aromatic hydrocarbons, as a function of the CC bond character that has been replaced by the BN unit. All values have been computed at the TD-B3LYP/6-311G(d,p) level of theory applied on equilibrium nuclear geometries obtained at the same level of theory. Energy differences are given in eV. Carbon hexagons highlighted with green rings correspond to aromatic sextets. In the case of phenanthrene we have included also substituted single bonds of opposite BN orientations, for the rest of the systems solely on BN orientations has been considered.

Summary

In this study, we have investigated the impact of incorporating boron-nitrogen (BN) units into polyaromatic hydrocarbons on their excited-state properties. Our results show that BN doping in positions of substantially weak electron delocalization (such as single bonds) leads to larger differences in the first singlet and triplet excitation energies than the pristine molecule. However, when the BN unit replaces double bonds or bonds belonging to aromatic sextets of high electron delocalization, less pronounced changes in the first singlet and triplet excitation energies are delivered. We have also observed a partial correlation between electron delocalization in bonds and excitation energies in species where one of their aromatic bonds has been substituted with a BN unit. Our findings provide valuable insights for designing and developing BN-doped polyaromatic hydrocarbons with customized photophysical properties.

Acknowledgements

Part of this work was granted access to the HPC resources of [CCRT/CINES/IDRIS] under the allocation 2022-2023 [AD010807031R1] made by GENCI (Grand Equipement National de Calcul Intensif). We also acknowledge the “Direction du Numérique” of the “Université de Pau et des Pays de l’Adour” for the computing facilities provided.

References

- [1] Z.X. Giustra, S.-Y. Liu, The State of the Art in Azaborine Chemistry: New Synthetic Methods and Applications, *J Am Chem Soc.* 140 (2018) 1184–1194. <https://doi.org/10.1021/jacs.7b09446>.
- [2] H. Helten, B=N Units as Part of Extended π -Conjugated Oligomers and Polymers, *Chemistry – A European Journal.* 22 (2016) 12972–12982. <https://doi.org/10.1002/chem.201602665>.
- [3] Y. Chen, W. Chen, Y. Qiao, X. Lu, G. Zhou, BN-Embedded Polycyclic Aromatic Hydrocarbon Oligomers: Synthesis, Aromaticity, and Reactivity, *Angewandte Chemie - International Edition.* 59 (2020) 7122–7130. <https://doi.org/10.1002/anie.202000556>.
- [4] Z. Liu, J.S.A. Ishibashi, C. Darrigan, A. Dargelos, A. Chrostowska, B. Li, M. Vasiliu, D.A. Dixon, S.Y. Liu, The Least Stable Isomer of BN Naphthalene: Toward Predictive Trends for the Optoelectronic Properties of BN Acenes, *J Am Chem Soc.* 139 (2017) 6082–6085. <https://doi.org/10.1021/jacs.7b02661>.
- [5] A. Chrostowska, S. Xu, A.N. Lamm, A. Mazière, C.D. Weber, A. Dargelos, P. Baylère, A. Graciaa, S.Y. Liu, UV-photoelectron spectroscopy of 1,2- and 1,3-azaborines: A combined experimental and computational electronic structure analysis, *J Am Chem Soc.* 134 (2012) 10279–10285. <https://doi.org/10.1021/ja303595z>.
- [6] S. Chakraborty, P. Kayastha, R. Ramakrishnan, The chemical space of B, N-substituted polycyclic aromatic hydrocarbons: Combinatorial enumeration and high-throughput first-principles modeling, *Journal of Chemical Physics.* 150 (2019). <https://doi.org/10.1063/1.5088083>.
- [7] J. Huang, Y. Li, BN Embedded Polycyclic π -Conjugated Systems: Synthesis, Optoelectronic Properties, and Photovoltaic Applications, *Front Chem.* 6 (2018). <https://doi.org/10.3389/fchem.2018.00341>.
- [8] P. Karamanis, N. Otero, D. Xenides, H. Denawi, M. Mandado, M. Rérat, From Pyridine Adduct of Borabenzene to (In)finite Graphene Architectures Functionalized with N \rightarrow B Dative Bonds. Prototype Systems of Strong One- and Two-Photon Quantum Transitions Triggering Large Nonlinear Optical Responses, *The Journal of Physical Chemistry C.* 124 (2020) 21063–21074. <https://doi.org/10.1021/acs.jpcc.0c05190>.
- [9] H. Huang, L. Liu, J. Wang, Y. Zhou, H. Hu, X. Ye, G. Liu, Z. Xu, H. Xu, W. Yang, Y. Wang, Y. Peng, P. Yang, J. Sun, P. Yan, X. Cao, B.Z. Tang, Aggregation caused quenching to aggregation induced emission transformation: a precise tuning based on BN-doped polycyclic aromatic hydrocarbons toward subcellular organelle specific imaging, *Chem Sci.* 13 (2022) 3129–3139. <https://doi.org/10.1039/D2SC00380E>.
- [10] P.G. Campbell, L.N. Zakharov, D.J. Grant, D.A. Dixon, S.-Y. Liu, Hydrogen Storage by Boron–Nitrogen Heterocycles: A Simple Route for Spent Fuel Regeneration, *J Am Chem Soc.* 132 (2010) 3289–3291. <https://doi.org/10.1021/ja9106622>.
- [11] T. Zeng, S.K. Møllerup, D. Yang, X. Wang, S. Wang, K. Stamplecoskie, Identifying (BN) 2-Pyrenes as a New Class of Singlet Fission Chromophores: Significance of Azaborine Substitution, n.d.
- [12] J.S.A. Ishibashi, A. Dargelos, C. Darrigan, A. Chrostowska, S.Y. Liu, BN Tetracene: Extending the Reach of BN/CC Isosterism in Acenes, *Organometallics.* 36 (2017) 2494–2497. https://doi.org/10.1021/ACS.ORGANOMET.7B00296/SUPPL_FILE/OM7B00296_SI_002.XYZ.

- [13] N. Otero, K.E. El-kelany, C. Pouchan, M. Rérat, P. Karamanis, Establishing the pivotal role of local aromaticity in the electronic properties of boron-nitride graphene lateral hybrids, *Physical Chemistry Chemical Physics*. 18 (2016) 25315–25328. <https://doi.org/10.1039/C6CP04502B>.
- [14] A. Mazière, A. Chrostowska, C. Darrigan, A. Dargelos, A. Graciaa, H. Chermette, Electronic structure of BN-aromatics: Choice of reliable computational tools, *J Chem Phys*. 147 (2017) 164306. <https://doi.org/10.1063/1.4993297>.
- [15] A. Abengózar, D. Sucunza, P. García-García, D. Sampedro, A. Pérez-Redondo, J.J. Vaquero, A New Member of the BN-Phenanthrene Family: Understanding the Role of the B - N Bond Position, *Journal of Organic Chemistry*. 84 (2019) 7113–7122. <https://doi.org/10.1021/acs.joc.9b00800>.
- [16] M.J. Frisch, G.W. Trucks, H.B. Schlegel, G.E. Scuseria, M.A. Robb, J.R. Cheeseman, G. Scalmani, V. Barone, G.A. Petersson, H. Nakatsuji, X. Li, M. Caricato, A. V. Marenich, J. Bloino, B.G. Janesko, R. Gomperts, B. Mennucci, H.P. Hratchian, J. V. Ortiz, A.F. Izmaylov, J.L. Sonnenberg, D. Williams-Young, F. Ding, F. Lipparini, F. Egidi, J. Goings, B. Peng, A. Petrone, T. Henderson, D. Ranasinghe, V.G. Zakrzewski, J. Gao, N. Rega, G. Zheng, W. Liang, M. Hada, M. Ehara, K. Toyota, R. Fukuda, J. Hasegawa, M. Ishida, T. Nakajima, Y. Honda, O. Kitao, H. Nakai, T. Vreven, K. Throssell, J.A. Montgomery Jr., J.E. Peralta, F. Ogliaro, M.J. Bearpark, J.J. Heyd, E.N. Brothers, K.N. Kudin, V.N. Staroverov, T.A. Keith, R. Kobayashi, J. Normand, K. Raghavachari, A.P. Rendell, J.C. Burant, S.S. Iyengar, J. Tomasi, M. Cossi, J.M. Millam, M. Klene, C. Adamo, R. Cammi, J.W. Ochterski, R.L. Martin, K. Morokuma, O. Farkas, J.B. Foresman, D.J. Fox, *Gaussian[™] 16 Revision C.01*, (2016).
- [17] T. Yanai, D.P. Tew, N.C. Handy, A new hybrid exchange–correlation functional using the Coulomb-attenuating method (CAM-B3LYP), *Chem Phys Lett*. 393 (2004) 51–57. <https://doi.org/10.1016/j.cplett.2004.06.011>.
- [18] H. Koch, P. Jørgensen, Coupled cluster response functions, *J Chem Phys*. 93 (1998) 3333. <https://doi.org/10.1063/1.458814>.
- [19] S. Hirata, M. Head-Gordon, Time-dependent density functional theory within the Tamm–Dancoff approximation, *Chem Phys Lett*. 314 (1999) 291–299. [https://doi.org/10.1016/S0009-2614\(99\)01149-5](https://doi.org/10.1016/S0009-2614(99)01149-5).
- [20] T.J. Lee, P.R. Taylor, A diagnostic for determining the quality of single-reference electron correlation methods, *Int J Quantum Chem*. 36 (1989) 199–207. <https://doi.org/10.1002/QUA.560360824>.
- [21] N. Otero, P. Karamanis, C. Pouchan, Hirshfeld-based atomic population analysis of the B, N doping effect in zigzag graphene nanoribbons: π electron density as requirement to follow the B, N doping guidelines, *Theor Chem Acc*. 137 (2018). <https://doi.org/10.1007/s00214-017-2189-5>.
- [22] N. Otero, C. Pouchan, P. Karamanis, Quadratic nonlinear optical (NLO) properties of borazino (B₃N₃)-doped nanographenes, *J Mater Chem C Mater*. 5 (2017). <https://doi.org/10.1039/c7tc01963g>.
- [23] P. Karamanis, N. Otero, C. Pouchan, Electric property variations in nanosized hexagonal boron nitride/graphene hybrids, *Journal of Physical Chemistry C*. 119 (2015). <https://doi.org/10.1021/acs.jpcc.5b02793>.
- [24] P. Bultinck, C. Van Alsenoy, P.W. Ayers, R. Carbó-Dorca, Critical analysis and extension of the Hirshfeld atoms in molecules, *Journal of Chemical Physics*. 126 (2007). <https://doi.org/10.1063/1.2715563>.
- [25] P. Bultinck, P.W. Ayers, S. Fias, K. Tiels, C. Van Alsenoy, Uniqueness and basis set dependence of iterative Hirshfeld charges, *Chem Phys Lett*. 444 (2007) 205–208. <https://doi.org/10.1016/j.cplett.2007.07.014>.
- [26] P. Karamanis, N. Otero, C. Pouchan, Electric Property Variations in Nanosized Hexagonal Boron Nitride/Graphene Hybrids, *The Journal of Physical Chemistry C*. 119 (2015) 11872–11885. <https://doi.org/10.1021/acs.jpcc.5b02793>.
- [27] M. Giambiagi, M.S. de Giambiagi, C.D. dos S. Silva, A.P. de Figueiredo, Multicenter bond indices as a measure of aromaticity, *Physical Chemistry Chemical Physics*. 2 (2000) 3381–3392. <https://doi.org/10.1039/B002009P>.
- [28] M. Mandado, M.J. González-Moa, R.A. Mosquera, Chemical graph theory and n-center electron delocalization indices: A study on polycyclic aromatic hydrocarbons, *J Comput Chem*. 28 (2007) 1625–1633. <https://doi.org/10.1002/jcc.20647>.

- [29] P. Bultinck, R. Ponec, S. Van Damme, Multicenter bond indices as a new measure of aromaticity in polycyclic aromatic hydrocarbons, *J Phys Org Chem.* 18 (2005) 706–718. <https://doi.org/10.1002/poc.922>.
- [30] M.M. N. Otero, NDELOC, (2022).
- [31] J. Poater, M. Duran, M. Solà, Aromaticity determines the relative stability of kinked vs. straight topologies in polycyclic aromatic hydrocarbons, *Front Chem.* 6 (2018) 561. <https://doi.org/10.3389/FCHEM.2018.00561/BIBTEX>.
- [32] M. Mandado, N. Otero, R.A. Mosquera, Local aromaticity study of heterocycles using n-center delocalization indices: the role of aromaticity on the relative stability of position isomers, *Tetrahedron.* 62 (2006) 12204–12210. <https://doi.org/10.1016/j.tet.2006.10.022>.
- [33] N. Otero, P. Karamanis, M. Mandado, A new method to analyze and understand molecular linear and nonlinear optical responses: Via field-induced functions: A straightforward alternative to sum-over-states (SOS) analysis, *Physical Chemistry Chemical Physics.* 21 (2019). <https://doi.org/10.1039/c8cp07362g>.
- [34] N. Otero, K.E. El-kelany, C. Pouchan, M. Rérat, P. Karamanis, Establishing the pivotal role of local aromaticity in the electronic properties of boron-nitride graphene lateral hybrids, *Physical Chemistry Chemical Physics.* 18 (2016) 25315–25328. <https://doi.org/10.1039/C6CP04502B>.
- [35] N. Otero, P. Karamanis, K.E. El-Kelany, M. Rérat, L. Maschio, B. Civalleri, B. Kirtman, Exploring the Linear Optical Properties of Borazine (B₃N₃) Doped Graphenes. 0D Flakes vs 2D Sheets, *The Journal of Physical Chemistry C.* 121 (2017) 709–722. <https://doi.org/10.1021/acs.jpcc.6b10837>.
- [36] M.B. Smith, J. Michl, Singlet Fission, *Chem Rev.* 110 (2010) 6891–6936. <https://doi.org/10.1021/cr1002613>.
- [37] T. Nagami, H. Miyamoto, W. Yoshida, K. Okada, T. Tonami, M. Nakano, Theoretical Molecular Design of Phenanthrenes for Singlet Fission by Diazadibora-Substitution, *J Phys Chem A.* 124 (2020) 6778–6789. <https://doi.org/10.1021/acs.jpca.0c05359>.
- [38] A.T. Balaban, P. v. R. Schleyer, H.S. Rzepa, Crocker, Not Armit and Robinson, Begat the Six Aromatic Electrons, *Chem Rev.* 105 (2005) 3436–3447. <https://doi.org/10.1021/cr0300946>.
- [39] J.W. Hager, S.C. Wallace, Two-Laser Photoionization Supersonic Jet Mass Spectrometry of Aromatic Molecules, *Anal Chem.* 60 (1988) 5–10. https://doi.org/10.1021/AC00152A003/ASSET/AC00152A003.FP.PNG_V03.
- [40] B. Saed, R. Omidyan, Electronically excited states of protonated aromatic hydrocarbons: Phenanthrene and pyrene, *Journal of Physical Chemistry A.* 117 (2013) 2499–2507. <https://doi.org/10.1021/jp400554h>.